Penerbit Akademia Baru

CFD Letters

Journal homepage: www.akademiabaru.com/cfdl.html
ISSN: 2180-1363

CFD Analysis on Course Stability of a Towed Ship Incorporated with Symmetrical Bridle Towline

Open Access

Ahmad Fitriadhy[1,*], Nur Adlina Aldin[1], Nurul Aqilah Mansor[1]

[1] Programme of Maritime Technology, Faculty of Ocean Engineering Technology and Informatics, Universiti Malaysia Terengganu, 21030 Kuala Terengganu, Terenggan, Malaysia

ARTICLE INFO

Article history:
Received 21 October 2019
Received in revised form 17 December 2019
Accepted 20 December 2019
Available online 30 December 2019

ABSTRACT

Instability of a towed ship presented in the form of her vigorous sway motions may be susceptible to a serious towing accident especially in the restricted waterways. To prevent such phenomenon occurs, a comprehensive investigation on course stability of a towed ship is obviously required. This paper presents Computational Fluid Dynamic (CFD) approach to analyze the course stability of the towed ship associated with symmetrical bridle towline configuration. Several towing parameters such as various towline lengths and towing's velocities have been taken into account in the computational simulation. Here, a towed ship was designated as 1B (barge) and employed in the simulations. The results revealed that the subsequent increase of the towline length has degraded the course stability of the towed ship, which imposed upon the increase of the sway motion of the towed ship by 1.95%. In addition to the increase of the towing's velocity from V_s=0.509 m/s up to 0.655 m/s, the course stability of the towed ship has led to the unstable towing condition indicated by 10.77% increment of the yaw motion. It can be concluded that the course stability of the towed barge is degraded, attributed by larger towline length and towing's velocity. These findings are beneficial and contribute to ship towing system safety navigation.

Keywords:
Course stability; sway motion; yaw motion; CFD; towing point and towline length

Copyright © 2019 PENERBIT AKADEMIA BARU - All rights reserved

1. Introduction

The drastic growth of shipping activities leads to heavy congestion due to abundant of ships in the waterways that threaten the safety navigation on the ship towing system. Even, it may cause monetary losses due to serious marine accidents [1]. Therefore, an extensive course stability investigation is then required to observe behavior of towed barge during the operations.

In recent years, researchers have presented numerous studies on investigating the course stability of the towed vessel [2-7]. Lee [8], Fitriadhy *et al.,* [2], and Fitriadhy *et al.,* [7] analysed the course stability of the towed vessel by means of the numerical analysis. Lee [8] stated that unsuitable length will induce larger amplitude motions and make it impossible to keep a towed barge in an equilibrium position. Fitriadhy *et al.,* [2] performed a numerical analysis on effect of different towline

* *Corresponding author.*
E-mail address: naoe.afit@gmail.com (Ahmad Fitriadhy)

length, tow point location on the barge and tug. The results showed that the increase of towline length and towing's point ratios have degraded the course stability of the towed barge due to excessive sway motion. Fitriadhy *et al.,* [7] proposed the subsequent increase of towline length resulted tended to have longer period motion which was proportional to the increment of amplitude of fishtailing motion. Zan *et al.,* have investigated the effect of different towline configuration to the course stability of the towed barge using the experimental approach [9]. They concluded that employing bridle towline configuration improved course stability of towed barge compared to single towline configuration. However, this experimental approach is relatively expensive, time consuming and impractical to be conducted. Hence, a reliable Computational Fluid Dynamics (CFD) approach is obviously flexible and adaptable than experiment, meanwhile the prediction result was more precise than the numerical approach.

This paper presents a CFD analysis on course stability of a towed ship incorporated with a symmetrical bridle towline configuration in calm water condition. Here, CFD simulation using Flow3D v11.2 software has been successfully conducted. Several parameters such as towline length and towing's velocities has been employed in the simulation, in which the course stability performance of the barge incorporated with the symmetrical bridle towline model has been discussed. The purpose of the study is to attain understanding on towed barge motions by considering three degree-of-freedom of the barge; surge, sway and yaw motion associated to dynamic towline tension. The CFD approach can provide truly available outcomes looking into a hydrodynamic description underlying the rationale behind the results explained.

2. Governing Equation

The CFD flow solver on Flow3D version 11.2 is based on the incompressible unsteady RANS equations in which the solver applies the Volume of Fluid (VOF) to track the free surface elevation. Besides, the solver can simulate free surface flows, viscous interactions and wave patterns [10]. Fractional area volume obstacle representation (FAVOR) is used to simulate the interface between fluid and solid boundaries. Open area and volume in each cell is computed by this method to define the area that is occupied by obstacle [11].

2.1 Continuity and Momentum Equation

The continuity and momentum equations for a moving object and the relative transport equation for VOF function are [11]

$$\frac{V_f}{\rho}\frac{\partial \rho}{\partial t} + \frac{1}{\rho}\nabla.\left(\rho \vec{u} A_f\right) = -\frac{\partial V_f}{\partial t} \tag{1}$$

$$\frac{\partial \vec{u}}{\partial t} + \frac{1}{V_f}\left(\vec{u}A_f.\nabla\vec{u}\right) = -\frac{1}{\rho}\left[\nabla_\rho + \nabla.\left(\tau A_f\right)\right] + \vec{G} \tag{2}$$

$$\frac{\partial F}{\partial t} + \frac{1}{V_f}\nabla.\left(F\vec{u}A_f\right) = -\frac{F}{V_f}\frac{\partial V_f}{\partial t} \tag{3}$$

where ρ is the density of the fluid, $\vec{u}$ is the fluid velocity, V_f is the volume fraction,A_f is the area fraction, p is the pressure, τ is the viscous stress tensor, G denotes gravity and F is the fluid fraction.

In the case of coupled GMO's motion, Eq. (1) and (2) are solved at each time step and the location of all moving objects is recorded and the area and volume fractions updated using the FAVOR technique. Eq. (3) are solved with the source term $\left(-\partial V_f/\partial t\right)$ which is computed as

$$-\frac{\partial V_f}{\partial t} = \vec{U}_{obj}\vec{n}S_{obj}/\,V_{cell} \tag{4}$$

where $S_{obj}$is the surface area, $\vec{n}$surface normal vector, $\vec{U}_{obj}$ is the velocity of the moving object at a mesh cell and $V_{cell}$is the total volume of the cell [11].

2.2 Turbulence Model

In this simulation, RNG k-ε turbulence model is employed in the simulation. This turbulence model was used for the simulation of the exchange flow between open water and floating object since it accounts for low Reynolds number effects [12-14] which applied the double averaging strategy to the transport equations for TKE and its dissipation rate produces the turbulence model for the flow. Referring to Flow 3D [11], the resulting equations are

$$\frac{\delta k}{\delta t} + U_j\frac{\delta k}{\delta x_j} = \frac{\delta}{\delta x_j}\left[\left(\nu + \frac{\nu_t}{\sigma_k}\right)\frac{\delta k}{\delta x_j}\right] + P_k + B_k + W_k - \varepsilon \tag{5}$$

$$\frac{\delta \varepsilon}{\delta t} + U_j\frac{\delta \varepsilon}{\delta x_j} = \frac{\delta}{\delta x_j}\left[\left(\nu + \frac{\nu_t}{\sigma_\varepsilon}\right)\frac{\delta \varepsilon}{\delta x_j}\right] + C_{1\varepsilon}\frac{\varepsilon}{k}(P_k + B_k)(1 + C_{3\varepsilon}R_f) + W_\varepsilon - C^*_{2\varepsilon}\frac{\varepsilon^2}{k} \tag{6}$$

$$P_k = \nu_t S^2 = \nu_t\left(\frac{\delta U_i}{\delta x_j} + \frac{\delta U_j}{\delta x_i}\right)\frac{\delta U_i}{\delta x_j} \tag{7}$$

$$B_k = \beta g_i\frac{\nu_t}{\sigma_s}\frac{\delta s}{\delta x_i} \tag{8}$$

where P_k is the shear production term of TKE, $S = \sqrt{2S_{ij}S_{ji}}$ is the modulus of the mean rate of strain tensor and $S_{ij} = 1/2(\delta U_i/\delta x_j + \delta U_j/\delta x_i)$, B_k is the buoyant production term of TKE, W_k is the wake production tern of TKE, W_ε is the wake production term in ε, σ_k and σ_ε are the turbulent Prandtl numbers for k and ε, and $C_{i\varepsilon}$, $C_{3\varepsilon}$ and $C^*_{2\varepsilon}$ are model coefficients.

2.3 Body Motion Computation

Flow3D utilized the body motion in a space-fixed Cartesian coordinate system. The governing equation of the six degree of freedom (DOF) of a rigid body motion can be expressed in this coordinate system as [11]

$$\frac{d}{dt}(m\vec{v}_c) = \vec{f} \tag{9}$$

$$\frac{d}{dt}(M_c.\vec{w}_c) = \vec{m}_c \tag{10}$$

The index C denotes the centre of mass of the body, *m* denotes the mass of the body, $\vec{v}_c$ the velocity vector, M_c is the tensor of the moments of inertia, $\vec{\omega}_c$ is the angular velocity vector, $\vec{f}$ denotes the

resulting force vector and $\vec{m}_c$ denotes the resultant moment vector acting on the body [12]c. The resultant force $\vec{f}$ has three components; surface force, field forces and external forces

$$\vec{f} = \int_S (T - \rho I).\vec{n}dS + \int_V \rho_b \vec{b}dV + \vec{f}E \quad (11)$$

Here, $\rho_b$is the density of the body. The only field force considered is the gravity, so the volume integral of above equation (right hand side) reduces to$m\vec{g}$, where g is the gravity acceleration vector. The vector $f\vec{E}$ denotes the external forces acting in the body [15].

3. Simulation Condition

3.1 Principal Data of Ship

The principal dimensions barge (1B) are presented in Table 1. The model and body plan of the barge is shown in Figure 1 and Figure 2, respectively.

Fig. 1. Model of barge

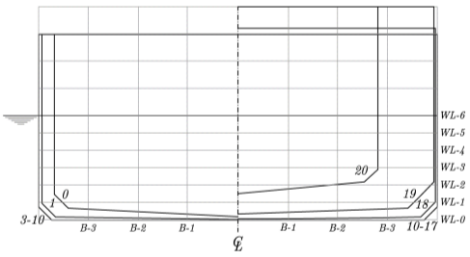

Fig. 2. Body plan of barge

Table 1
Principal dimensions of barge (1B)

	1B	
Description	Full-scale	Model
Length, L(m)	60.96	1.219
Breadth, B(m)	10.67	0.213
Draft, d(m)	2.74	0.0548
Volume, V(m^3)	1646.2	0.01317
L/B	5.71	5.71
Block coefficient,C_b	0.92	0.92
k_{yy2}/L	0.3266	0.3266
$X_{G\ abaft\ the\ midship}$,(m)	-1.04	-0.0208

3.2 Parametric Studies

In the simulation several towline lengths, l', towing's velocity, V_s and towing have been employed in the simulation as completely summarised in Table 2 and Table 3, respectively, where the towing point location, l'_b is assumed as constant, where l'_b=0.5.

Table 2
Various towline length, l'

Towline length, l'	Towing velocity, $V_s(\frac{m}{s})$
1.0 L	
2.0 L	0.509
3.0 L	

Table 3
Various towing velocity, V_s

Towline length, l'	Towing velocity, $V_s(\frac{m}{s})$
1.0 L	0.509
	0.582
	0.655

3.3 Computational Domain and Boundary Conditions

The computational domain and the boundary conditions of the simulation displayed clearly in Figure 3. Referring to Table 4, specified velocity and specified pressure boundary type condition is assigned to allow water flow and apply hydrostatic pressure to the domain, respectively. In addition, the outflow boundary condition is allocated to prevent wave reflection into the domain. Furthermore, the meshing generation is created in Flow3D as shown in Figure 4. The barge or the towed ship is coupled to the virtual tug via a towline. Here, the virtual tug is modelled as the sphere model and assigned as prescribed motion. Meanwhile the surge, sway and yaw motions of the barge was set as the coupled motion. The barge was initially inclines by 15° to starboard side. In addition, the towline is set as mass-less rope with spring coefficient of $0.787 N/m^2$.

Table 4
Computation domain simulation

Boundary	Mesh block
X_{min}	Specified velocity
X_{max}	Outflow
Y_{min}	Outflow
Y_{max}	Outflow
Z_{min}	Symmetry
Z_{max}	Specified pressure

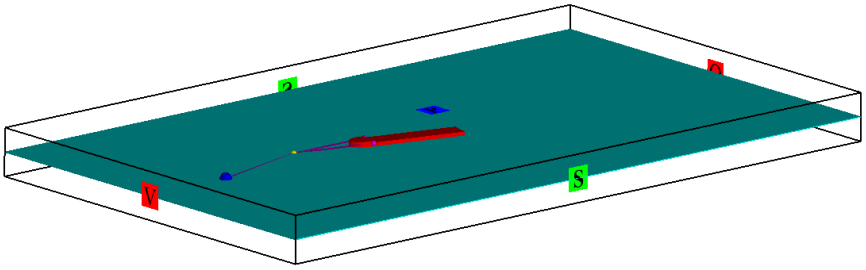

Fig. 3. Boundary conditions

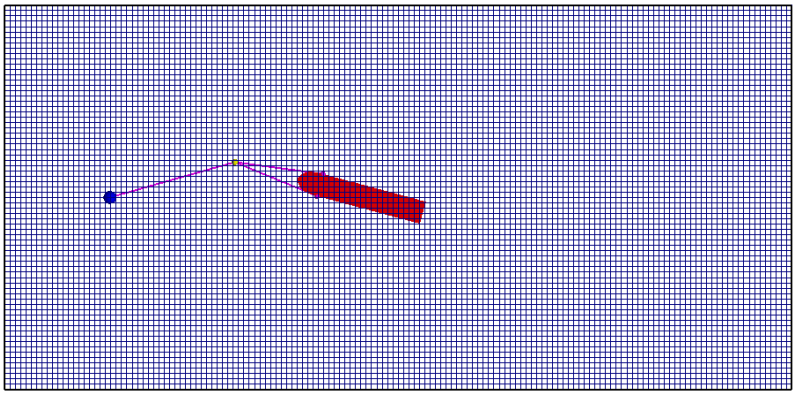

Fig. 4. Meshing generation

The CFD simulations were successfully carried out in maritime technology simulation lab. For every simulation, the average duration was about 70-80 hours (4 parallel computations) on a HP Z820 workstation PC with processor Intel (R) Xeon (R) CPU ES-2690 v2 @ 3.00 GHz (2 processors) associated with the installed memory (RAM) of 32.0 GB and 64-bit Operating System.

3.4 Mesh Independent Study

Mesh independent study is necessary to determine an acceptable number of mesh with respect to steadiness in the computational simulation results. The results are completely presented in Table 5. Referring to the results, the total numbers of cells of 995,841 (case C) is then set from whole simulation cases associated with less computational time. This can be explained by the fact that the increase of total number of real cells up to 1,258,008 was unnecessary due to its insignificant influence into the computational results of the sway motion (see Figure 5).

Table 5
Mesh independent study at various number of cells

Case	Total number of real cells	Maximum sway motion (m)
A	503, 880	0.5665
B	743,850	0.6706
C	995,841	0.6265
D	1,258,008	0.7700

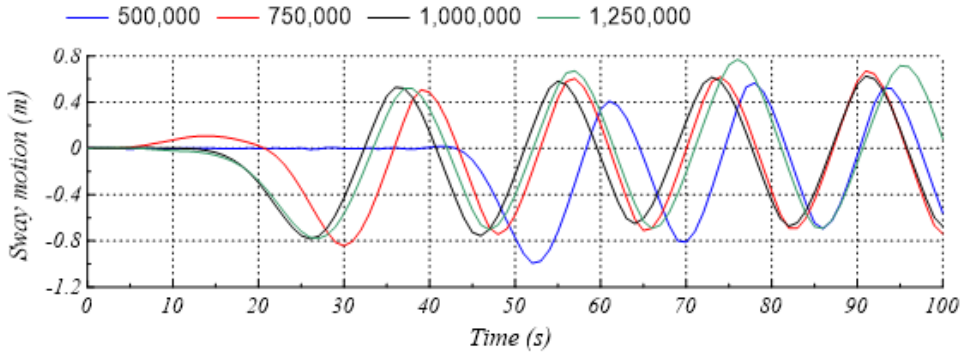

Fig. 5. Sway motion characteristics at various number of cells

4. Results and Discussions

The Computational Fluid Dynamic simulations have been successfully carried out to predict the course stability of the towing system in the various towline lengths and towing's velocity as displayed in Figures 6~9. The simulations results of the sway and yaw motion characteristics of the barge associated with the towline tension are appropriately discussed.

4.1 Effect of Towline Length

The characteristic of the sway motions at various towline lengths are displayed in Figure 6. Similar to what was reported by Fitriadhy *et al.,* [16], the sway motion amplitude has increased by 1.95% as the towline increased from l^t=1.0 up to l^t=3.0. Meanwhile, the fishtailing period of 1B has increased by 5.13% (see Table 6). Here, the effect of the extending towline was insignificant to the magnitude of the yaw motions. A possible reason for this may rest with the less towing velocity condition. In addition, the towline tension appeared to be insignificant as the towline length increased as also

stated by Fitriadhy and Yasukawa [2]. The further increase of towline length has resulted in higher wave crest (red colour) at the barge's bow as shown in Figure 7. This reason can be explained by the fact that the increase of pressure and resistance acted on the barge which consequently increase the oscillation of sway motion during towing.

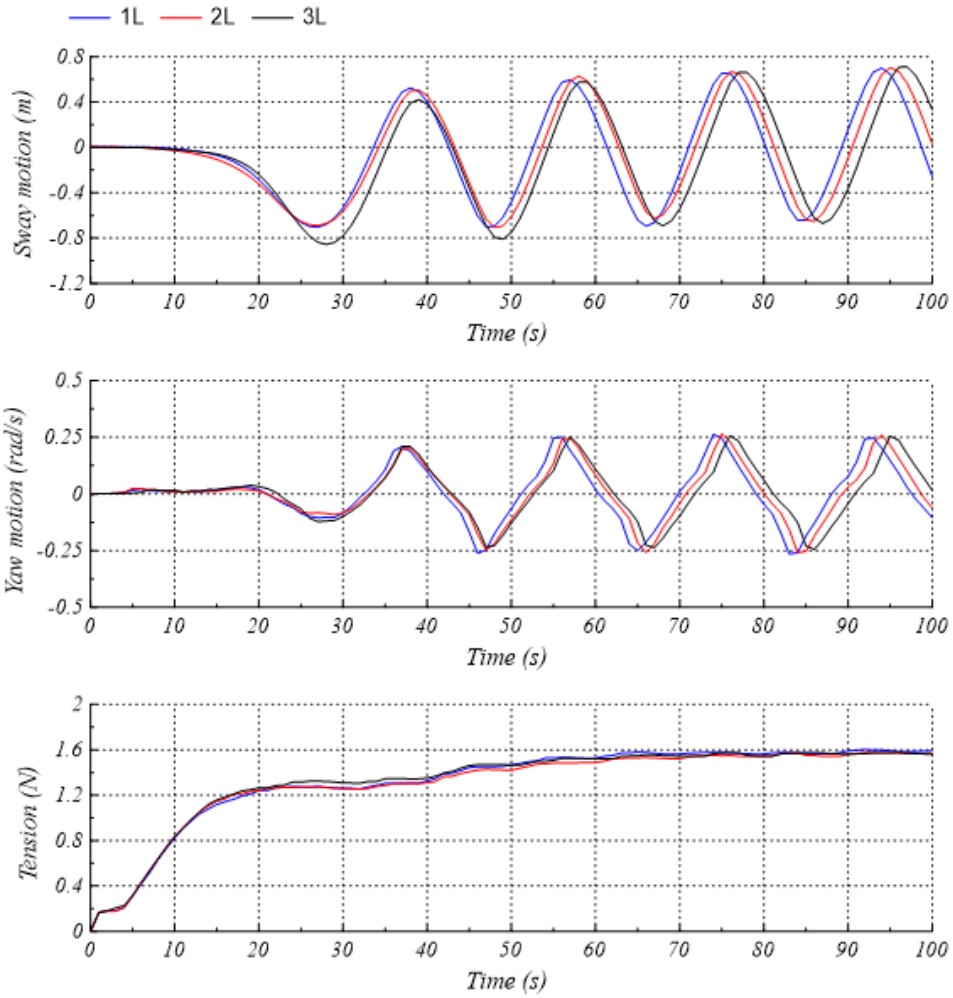

Fig. 6. Characteristics of sway and yaw motion of 1B associated with the towline tension at various towline lengths

Table 6
Period of sway motion at various towline lengths

Towline length, l^t	Period of sway motion	Percentage of increment (%)
1.0 L	18.5	-
2.0 L	19	2.63%
3.0 L	19.5	2.56%

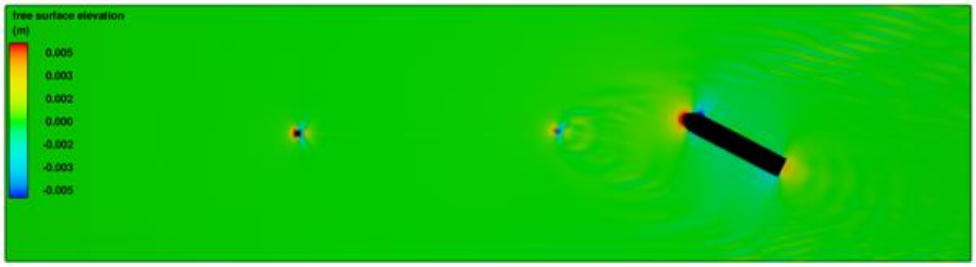

(a)

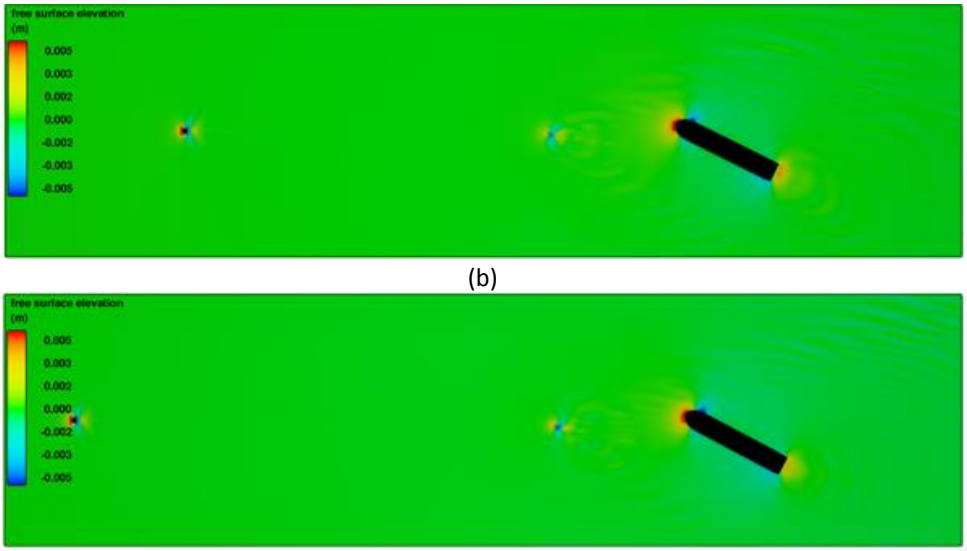

(b)

(c)

Fig. 7. Free surface elevation, Vs= 0.509, l' = (a) 1.0 L, (b) 2.0 L, and (c) 3.0 L (c)

4.2 Effect of Towing's Velocity

Figure 8 shows the characteristics of the sway and yaw motions associated with dynamic towline tension at various towing velocity. The subsequent increased of towing velocity from 0.509 m/s to 0.655 m/s resulted in sufficient increment of the sway motion of the barge by 13.69%. As seen, the increase of the towing velocity up to 0.655 m/s has been susceptible to the increase of the sway motion amplitude of the barge by 0.73 m. This means that the course stability of the barge has degraded. In addition, the period of the sway motion of the barge is inversely proportional with the increase of the towing velocity as summarised in Table 7. Besides, the yaw motion of the barge increased by 9.43% and 1.48% as the towing velocity increased from 0.509 to 0.582 m/s and 0.655 m/s, respectively. In addition, the magnitude of the towline tension has proportionally increased with respect to the towing velocity, where the maximum towline tension has reached by 2.449 N at the towing velocity of 0.655 m/s. Inherently, the maximum percentage of the towline tension increment is 19.81% (see Table 7). The reason can be explained by the fact that the wave elevation indicated by red colour at the bow region of the barge has been getting higher as compared to the towing velocity of 0.509 m/s and 0.582 m/s as displayed in Figure 9.

Table 7
Characteristics of sway motion and maximum tension at various towing velocities

Towing velocity, Vs	Period of sway motion	Maximum tension (N)	Percentage of increment (%)
0.509	18	1.608	-
0.582	16.5	2.006	19.81
0.655	15	2.449	18.10

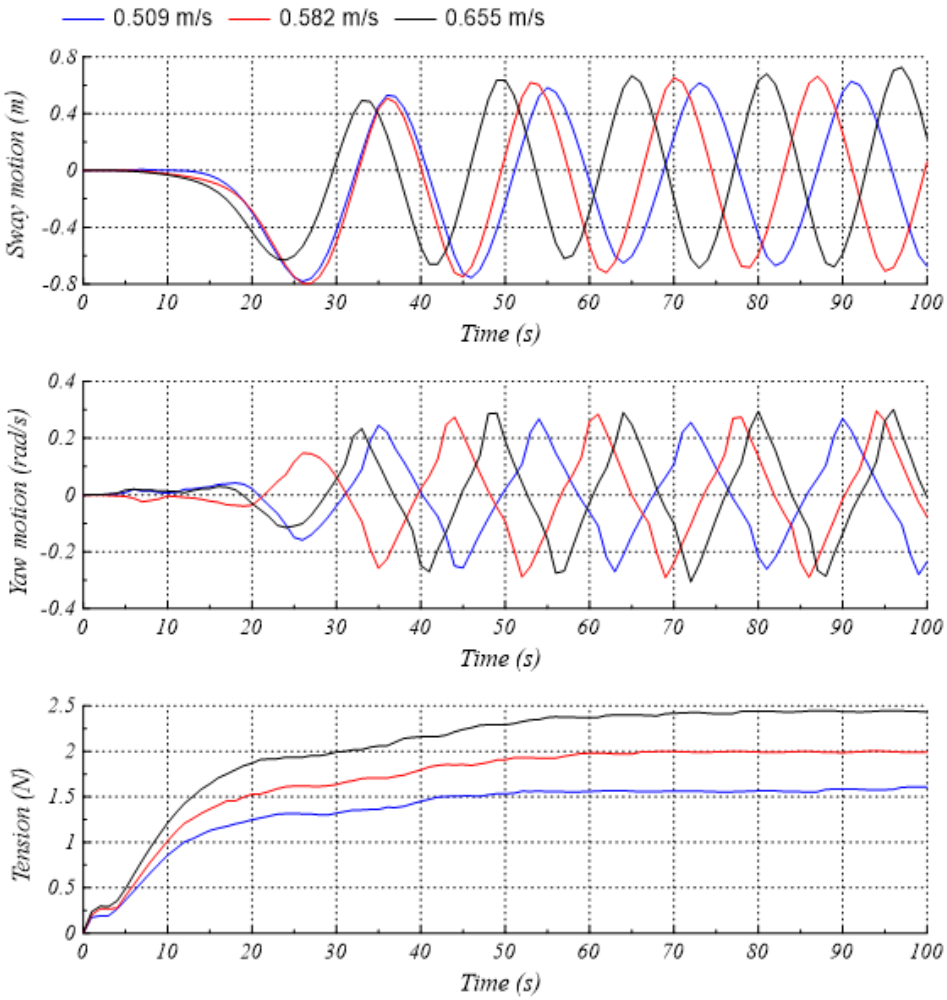

Fig. 8. Characteristics of sway and yaw motion of 1B associated with towline tension at various towing's velocity

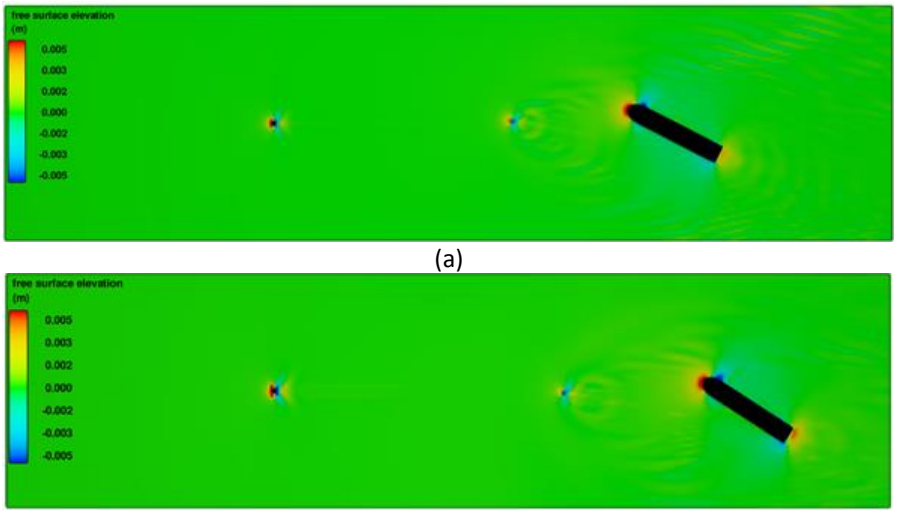

(a)

(b)

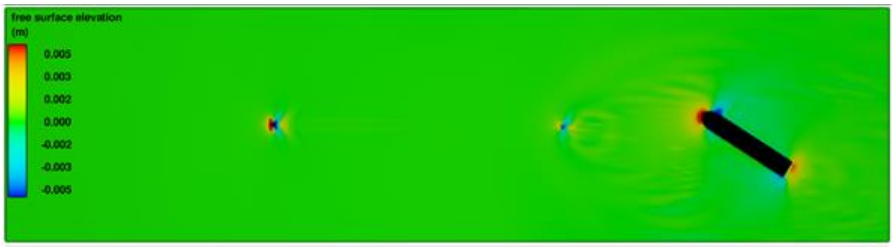

(c)

Fig. 9. Free surface elevation, Vs= (a) 0.509, (b) 0.582, and (c) 0.653 m/s

5. Conclusion

The Computational Fluid Dynamics (CFD) analysis on the course stability of the ship's towing system has been successfully carried out using Flow3D software. The effects of various towline lengths and towings velocities have been investigated. The conclusion results can be drawn as follows

a) Extending towline length, l'=1.0 to 3.0 degrades the course stability of the barge presented in the form of the increase of the sway and yaw motions. In general, the subsequent increase the towline length results in insignificant effect to the magnitude of the towline tension.
b) The increase of towing velocity from 0.509 m/s up to 0.655 m/s is proportional with the increase of the yaw motion of the barge by 10.77%. Meanwhile, the maximum towline tension is obtained by 34.32% as the towing velocity increases from 0.509 m/s to 0.655 m/s. The possible reason for this may occur due to the increase of resistance that can be seen at the higher wave elevation at the bow and stern region of the barge.

Acknowledgement

The authors greatly appreciate to Ministry Higher Education of Malaysia for the financial support awarded from Fundamental Research Grant Scheme (FRGS) Vot No. 59414.

References

[1] You, Youngjun, Jaewook Hur, and Junhyung Jung. "An experimental study on an auxiliary towing system for an FPSO using active thrusters." *Applied Ocean Research* 52 (2015): 62-72.
[2] Fitriadhy, Ahmad, and Hironori Yasukawa. "Course stability of a ship towing system." *Ship Technology Research* 58, no. 1 (2011): 4-23.
[3] Fitriadhy, Ahmad, and Hironori Yasukawa. "Turning ability of a ship towing system." *Ship Technology Research* 58, no. 2 (2011): 112-124.
[4] Fitriadhy, A., H. Yasukawa, and K. K. Koh. "Course stability of a ship towing system in wind." *Ocean Engineering* 64 (2013): 135-145.
[5] Fitriadhy, A., H. Yasukawa, T. Yoneda, K. K. Koh, and A. Maimun. "Analysis of an asymmetrical bridle towline model to stabilise towing performance of a towed ship." *Jurnal Teknologi* 66, no. 2 (2013)): 151-156.
[6] Fitriadhy, A., H. Yasukawa, and A. Maimun. "Theoretical and experimental analysis of a slack towline motion on tug-towed ship during turning." *Ocean Engineering* 99 (2015): 95-106.
[7] Fitriadhy, A., H. Yasukawa, W. B. W. Nik, and A. A. Bakar. "Numerical Simulation of Predicting Dynamic Towline Tension on a Towed Marine Vehicle." In *International Conference on Ships and Offshore Structures ICSOS*, vol. 31. 2016.
[8] Lee, Ming-Ling. "Dynamic stability of nonlinear barge-towing system." *Applied mathematical modelling* 13, no. 12 (1989): 693-701.
[9] Zan, U. I., H. Yasukawa, K. K. Koh, and A. Fitriadhy. "MODEL EXPERIMENTAL STUDY OF A TOWED SHIP'S MOTION." The 6th Asia-Pacific Workshop on Marine Hydrodymics-APHydro, 2012.
[10] Arifah Ali, Adi Maimun, and Yasser Mohamed Ahmed. "Analysis of Resistance and Generated Wave around Semi SWATH Hull at Deep and Shallow Water." *Journal of Advanced Research in Fluid Mechanics and Thermal Sciences* 58, no. 2 (2019): 247-260.

[11] *FLOW-3D 10.1.1 User Manual*. Flow Science Inc. 2013.
[12] Yakhot, Victor, and Steven A. Orszag. "Renormalization group analysis of turbulence. I. Basic theory." *Journal of scientific computing* 1, no. 1 (1986): 3-51.
[13] Yakhot, A., S. Rakib, and W. S. Flannery. "Low-Reynolds number approximation for turbulent eddy viscosity." *Journal of Scientific Computing* 9, no. 3 (1994): 283-292.
[14] Koutsourakis, Nektarios, John G. Bartzis, and Nicolas C. Markatos. "Evaluation of Reynolds stress, k-ε and RNG k-ε turbulence models in street canyon flows using various experimental datasets." *Environmental fluid mechanics* 12, no. 4 (2012): 379-403.
[15] Sisong, Yen, and Huang Genyu. "Dynamic performance of towing system-simulation and model experiment." In *OCEANS 96 MTS/IEEE Conference Proceedings. The Coastal Ocean-Prospects for the 21st Century*, vol. 1, pp. 216-230. IEEE, 1996.
[16] Fitriadhy, A., M. K. Aswad, N. Adlina Aldin, N. Aqilah Mansor, A. A. Bakar, and W. B. Nik. "Computational fluid dynamics analysis on the course stability of a towed ship." *Journal of Mechanical Engineering and Sciences* 11, no. 3 (2017): 2919-2929.